MOLECULAR AND CELLULAR BIOLOGY, June 2005, p. 4946–4955 Vol. 25, No. 12
0270-7306/05/$08.00+0 doi:10.1128/MCB.25.12.4946–4955.2005


# Reduced Affinity to and Inhibition by DKK1 Form a Common Mechanism by Which High Bone Mass-Associated Missense Mutations in LRP5 Affect Canonical Wnt Signaling

Minrong Ai,[1] Sheri L. Holmen,[2] Wim Van Hul,[3] Bart O. Williams,[2] and Matthew L. Warman[1]*

*Department of Genetics and Center for Human Genetics, Case School of Medicine and University Hospitals of Cleveland, Cleveland, Ohio[1]; Laboratory of Cell Signaling and Carcinogenesis, Van Andel Research Institute, Grand Rapids, Michigan[2]; and Department of Medical Genetics, University and University Hospital of Antwerp, Antwerp, Belgium[3]*

Received 7 January 2005/Returned for modification 21 January 2005/Accepted 16 March 2005

**The low-density-lipoprotein receptor-related protein 5 (LRP5), a coreceptor in the canonical Wnt signaling pathway, has been implicated in human disorders of low and high bone mass. Loss-of-function mutations cause the autosomal recessive osteoporosis-pseudoglioma syndrome, and heterozygous missense mutations in families segregating autosomal dominant high bone mass (HBM) phenotypes have been identified. We expressed seven different HBM-LRP5 missense mutations to delineate the mechanism by which they alter Wnt signaling. None of the mutations caused activation of the receptor in the absence of ligand. Each mutant receptor was able to reach the cell surface, albeit at differing amounts, and transduce exogenously supplied Wnt1 and Wnt3a signal. All HBM mutant proteins had reduced physical interaction with and reduced inhibition by DKK1. These data suggest that HBM mutant proteins can transit to the cell surface in sufficient quantity to transduce Wnt signal and that the likely mechanism for the HBM mutations' physiologic effects is via reduced affinity to and inhibition by DKK1.**

Low-density-lipoprotein receptor-related protein 5 (LRP5) is a single-pass transmembrane protein that belongs to the low-density-lipoprotein receptor superfamily. One function of LRP5 is to serve as a coreceptor in the canonical Wnt signaling cascade (8). Several in vitro observations support this function. For example, LRP5 transduced Wnt signal in cultured cells, and decoy forms of LRP5 could interfere with Wnt signaling (7). Additionally, yeast two-hybrid experiments identified Axin, a cytoplasmic component of the canonical signaling cascade, as being an LRP5-interacting partner (24). In vivo support for a role in Wnt signaling comes from studies of *Xenopus laevis* in which LRP5 was shown to synergize with Wnt to induce secondary axis formation (29). Furthermore, two closely related homologs of LRP5, arrow in *Drosophila melanogaster* and LRP6 in vertebrates, have also been shown to transduce Wnt signal (29, 33), and genetic interaction between LRP5 and LRP6, with respect to limb patterning, in mice has been observed (9, 18).

For humans, two disorders affecting bone mass have been associated with mutations in LRP5. Loss-of-function mutations cause the autosomal recessive osteoporosis-pseudoglioma syndrome (OPPG) (7). Individuals with this disease have skeletal fragility, due to low bone mass, and blindness, due to impaired blood vessel regression. The second skeletal phenotype associated with LRP5 mutation is autosomal dominant high bone mass (HBM), which is caused by heterozygous missense mutations (Fig. 1) (4, 21, 32). Affected individuals in families segregating HBM can develop complications associated with excessive bone formation, such as cranial nerve compression and severe headache (34); however, they have markedly reduced risks of skeletal fracture. OPPG and HBM phenotypes have been suggested to result from altered Wnt signaling (16). Skeletal phenotypes have also been noted when other Wnt signaling components have been altered. Disruption of secreted Frizzled-related protein 1, a secreted Wnt antagonist, causes high bone mass in mice (3). Increased production of DKK1, a canonical Wnt signaling inhibitor, by myeloma cells has been shown to correlate with bone lesions in patients with multiple myeloma (30). Tissue-specific deletion of β-catenin in skeletal precursor cells in developing mice leads to complete failure of osteoblast differentiation (12). Transgenic mice that overexpress Wnt10b in bone marrow mesenchymal progenitor cells have significantly increased bone mass, while Wnt10b null mice exhibit decreased bone mass (2). Alterations in bone mass have also been observed in mice with osteoblast-specific deletions of β-catenin or Apc, with the former having low bone mass and the latter increased bone mass (10a). Additionally, reduced bone mass in mice having osteoblast-specific overexpression of Dkk-1 has been reported in abstract form (20a). Finally, introduction of a single Lrp6 null allele onto a Lrp5 knockout background further reduced bone mineral density in mice (9), suggesting that Lrp5 and Lrp6 have partially overlapping roles in determining bone mass.

The types of mutations that cause OPPG are consistent with this phenotype being due to loss of LRP5 function. Disease alleles commonly involve nonsense and frameshift mutations, and OPPG-associated missense mutations fail to transduce Wnt signal in cell culture assays (7; our unpublished data). However, not all LRP5 missense mutations negatively affect Wnt signaling, since seven different mutations in families segregating HBM phenotypes have been described. Only one

* Corresponding author. Mailing address: Department of Genetics, BRB-719, Case School of Medicine, 2109 Adelbert Road, Cleveland, OH 44106. Phone: (216) 368-4919. Fax: (216) 368-5857. E-mail: mlw14@case.edu.

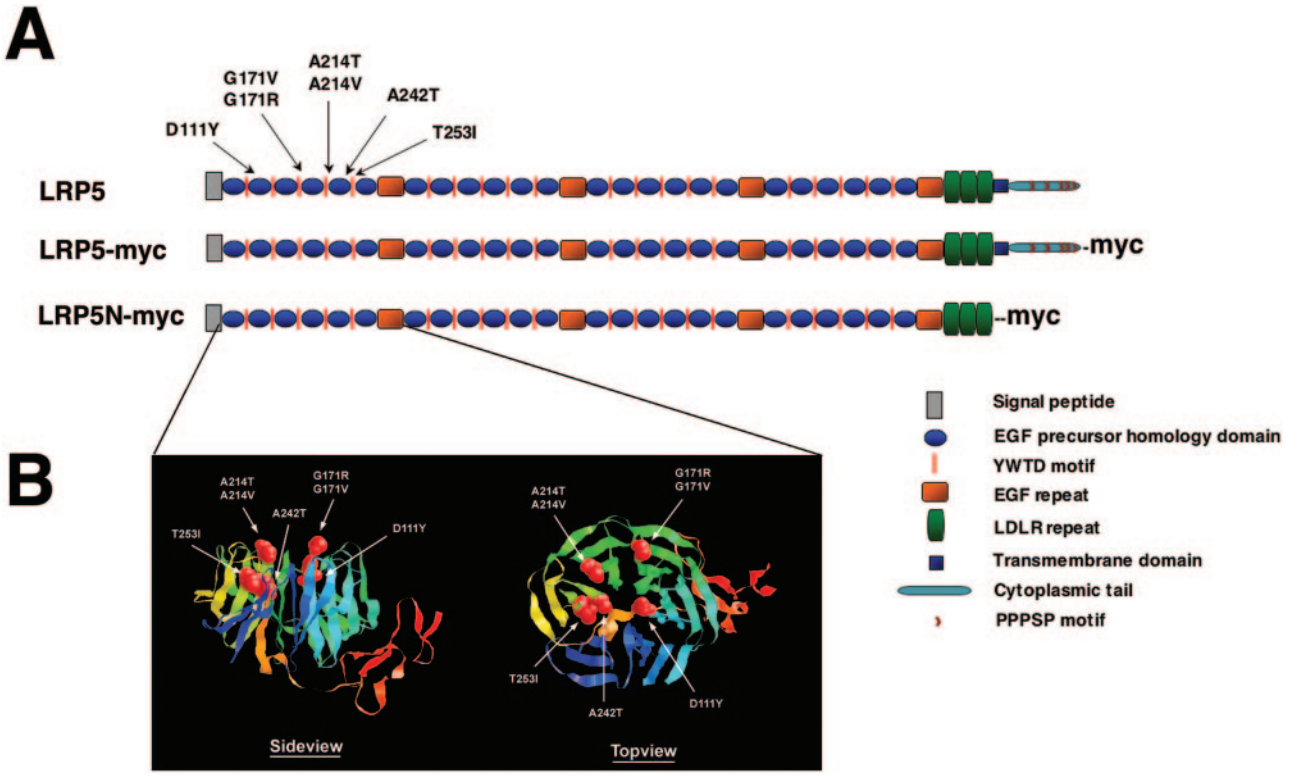


FIG. 1. Schematic of LRP5 expression constructs and sites of HBM-associated missense mutations. (A) WT and high bone mass-associated mutant LRP5 protein expression constructs. Each construct contained either a WT sequence or a single HBM-associated mutation. Specific amino acid mutations (in single-letter code) and their relative locations within the first EGF-like domain of LRP5 are noted. Constructs were full-length, untagged LRP5, full-length LRP5 that was tagged at the carboxy terminus with a myc-epitope (LRP5-myc), truncated LRP5 protein lacking the transmembrane and cytoplasmic domains but tagged at the carboxy terminus with a myc-epitope (LRP5N-myc). (B) Locations of the HBM mutations modeled on the three-dimensional structure of the EGF-like domain of the low-density-lipoprotein receptor (14) by using the RasMol molecular graphics visualization tool (version 2.6, September 1996 update [http://www.umass.edu/microbio/rasmol/getras.htm]; R. Sayle, Stevanage, United Kingdom). Note that all mutations affect residues near the top surface (side view) and central region (top view) of the β-propeller structure within the EGF-like domain.

HBM mutation (G171V) has been studied in vitro (4, 37). When transiently transfected into cells, the G171V mutant LRP5 protein was not constitutively active and did not transduce Wnt signal at levels greater than the wild-type (WT) levels (4); however, the mutant LRP5 protein was less efficiently inhibited by an endogenous inhibitor of LRP5 signaling, DKK1 (4). This led to the suggestion that the G171V-associated HBM phenotype was caused by reduced inhibition of LRP5 signaling during anabolic bone formation. More recently, a mechanism for reduced DKK1 inhibition was proposed when the G171V mutant was shown to transit poorly to the cell surface and not interact with the LRP5 intracellular chaperone MESD (37). These results implied that the HBM phenotype was caused by autocrine, intracellular signaling between Wnt ligand and mutant LRP5 that is retained within the endoplasmic reticulum and is not accessible to extracellular DKK1.

Here we report functional studies that utilized seven different HBM-causing missense mutations (Fig. 1), which we performed to determine how they affect Wnt signaling. We found that none of the HBM mutations were active in the absence of added Wnt. Even though different HBM mutant proteins transited the cell and reached the surface with differing efficiencies, all were able to transduce exogenously applied Wnt at levels comparable to those for WT-LRP5. However, compared to WT-LRP5, all of the HBM mutants were less inhibited by exogenously applied DKK1 protein and had reduced physical interaction with DKK1. We conclude that autocrine activation of Wnt signaling is not likely to be the general mechanism by which all missense mutations in LRP5 result in HBM phenotypes. Instead, our data support diminished regulation of the pathway by endogenous inhibitors, such as DKK1, as the most consistent mechanism for each of the HBM mutation's effects.

## MATERIALS AND METHODS

**Expression constructs for LRP5, MESD, and DKK1.** Full-length human WT-LRP5, full-length human WT-LRP5 that has a myc epitope at the carboxy terminus (WT-LRP5-myc), and a truncated form of human WT-LRP5 that lacks the transmembrane and cytoplasmic domains but has a myc epitope at the carboxy terminus (WT-LRP5N-myc) were cloned into the pcDNA3.1 expression vector (Invitrogen) as previously described (Fig. 1) (7). Seven different HBM-causing missense mutations and one mutation (T173M) that has been associated with autosomal dominant familial exudative vitreoretinopathy (31) were individually introduced into a 1.3-kb EcoRI/SalI restriction fragment containing the first epidermal growth factor-like (EGF-like) domain by site-directed mutagenesis (Quikchange; Stratagene). After it was confirmed that only the expected mutation and no other alteration was present within the mutated 1.3-kb fragment, the

fragment was then shuttled into the LRP5, LRP5-myc, and LRP5N-myc expression vectors.

To generate the expression construct containing the entire extracellular domain of human LRP6 fused to the constant region of the mouse immunoglobulin G (IgG) heavy chain (LRP6N-Fc), the sequence encoding the entire human LRP6 extracellular domain was cloned into N-LRP6-mIgG (described in reference 10) to generate LRP6N-Fc. The G158V mutant of LRP6N-Fc, which is equivalent to G171V in LRP5, was generated by site-directed mutagenesis and sequence verified.

To generate a carboxy-terminal V5-tagged version of mouse Wnt1, the gene was PCR amplified from cDNA. The forward primer attached a HindIII restriction site, and the reverse primer eliminated the stop codon and inserted an EcoRI restriction site. The PCR product was cloned into the TOPO Blunt vector (Invitrogen) to generate TOPO-mWnt1. This vector was sequenced to verify the amplified product. The TOPO-mWnt1 vector was digested with HindIII and EcoRI, and the mWnt1 fragment was cloned into the pcDNA6-V5/His expression plasmid (Invitrogen) to generate mWnt1-V5.

Xi He provided a Flag-tagged human DKK1 construct (27) that we subcloned into pcDNA3.1. DKK1-V5 was made by PCR amplifying DKK1 cDNA and cloning it into the pcDNA3.1-V5/His expression vector (Invitrogen). Bernadette Holdener provided mouse MESD-C2 and RAP expression constructs (11). Ormond MacDougald provided a mouse Wnt10b construct (2), which we subcloned into pcDNA3.1. Hans Clever provided the Topflash reporter construct (20). A *Renilla* luciferase construct, pRL-TK, was purchased (Upstate Biotechnology).

**Cell culture, expression of LRP5, LRP6, and DKK1, and collection of conditioned media.** HEK293T cells and Cos7 cells (American Type Culture Collection) were cultured in Dulbecco's modified Eagle's medium (DMEM) (Cellgro) with 10% fetal bovine serum (FBS) (Gibco-BRL). Conditioned medium (CM) containing DKK1-Flag (DKK1-CM) and conditioned medium from empty-vector-transfected cells (pcDNA3-CM) were generated by transiently transfecting 80% confluent 293T cells in six-well plates by use of Lipofectamine Plus (Invitrogen), following the manufacturer's protocol. Twenty-four hours after transfection, the culture medium was changed to 1 ml serum-free DMEM. Conditioned medium was collected 24 h later and stored frozen at −80°C until use.

LRP5N-myc recombinant protein was expressed in Cos7 or 293T cells. Cells were plated at $2 \times 10^5$ cells per well in six-well culture plates 24 h prior to transfection. Cos7 cells were transfected with 0.2 μg each of LRP5N-myc, MESD-C2, and RAP expression vectors by use of FuGENE 6 (Roche) following the manufacturer's protocol, while 293T cells were transfected by use of Lipofectamine Plus. Twenty-four hours after transfection, the culture medium was changed to serum-free DMEM. Conditioned medium was then collected 24 h later. Two percent of conditioned media and 2% of cell lysate were analyzed by immunoblot following reducing SDS-PAGE.

Control Rat2 cells and Rat2 cells stably expressing Wnt1 were provided by Anthony Brown (6). These cells were cultured in DMEM containing 10% FBS and Geneticin (50 μg/ml). Control L cells and L cells stably expressing Wnt3a were obtained from the American Type Culture Collection. These cells were also cultured in DMEM containing 10% FBS and Geneticin (50 μg/ml).

**Biotinylation of cell surface protein and immunodetection of biotinylated LRP5.** Cos7 cells were cultured in DMEM containing 10% FBS in 60-mm plates and, when 80% confluent, were transfected with 1.2 μg full-length LRP5-myc and 0.8 μg MESD-C2 expression vectors by use of the FuGENE 6, following the manufacturer's protocol. Forty-eight hours after transfection, cells were washed three times with ice-cold phosphate-buffered saline (PBS). Cells were incubated with PBS containing 0.5 mg/ml Sulfo-NHS-LC-Biotin (Pierce) at 4°C for 20 min. As a negative control, transfected cells were treated with PBS lacking the biotin-cross-linker at 4°C for 20 min. The labeling reaction was stopped by three washes of chilled PBS containing 50 mM $NH_4Cl$ at 4°C. Cells were lysed in 1 ml radioimmunoprecipitation assay (RIPA) buffer (50 mM Tris, pH 8, 150 mM NaCl, 1% NP-40, 0.5% deoxycholate, 0.1% sodium dodecyl sulfate). Biotin-labeled proteins were affinity purified from 0.4 ml cell lysate mixed with 0.5 ml RIPA buffer by use of 50 μl streptavidin beads (Pierce). Samples were then resuspended in 40 μl 2× SDS-PAGE loading buffer, and 20 μl was resolved by sodium dodecyl sulfate-polyacrylamide gel electrophoresis (SDS-PAGE) under reducing conditions (5% β-mercaptoethanol [BME]). Following transfer onto polyvinylidene difluoride (PVDF) membrane, LRP5-myc was immunodetected by use of a monoclonal anti-myc antibody, 9E10 (Santa Cruz Biotechnology, Inc.). As a positive control for cell surface biotinylation, β1 integrin was immunodetected by using a monoclonal antibody MAB2252Z (Chemicon). Secondary antibody was horseradish peroxidase (HRP)-conjugated anti-mouse IgG. Immunopositive bands were visualized by chemiluminescence using the ECL-Plus Western detection system (Amersham).

**Luciferase reporter assays for canonical Wnt signaling and immunodetection of LRP5 protein.** Each experiment was performed in triplicate and was repeated independently on at least three separate occasions.

**Assays involving 293T cells cotransfected with LRP5 and Wnt1-V5 or Wnt10b.** 293T cells were plated at $2.5 \times 10^5$ cells/well in 24-well plates 24 h prior to transfection. Cells were transfected by use of Lipofectamine Plus with Topflash reporter construct (100 ng), pRL-TK (5 ng), MESD-C2 (20 ng), Wnt1-V5 (100 ng) or Wnt10b (100 ng), and full-length, untagged LRP5 (20 ng) expression vectors in 250 μl serum-free medium according to the manufacturer's protocol. As needed, empty pcDNA3.1 vector was added to make the total transfected DNA amount 250 ng. Four hours later, an additional 250 μl of DMEM containing 20% FBS was added to the cells. When DKK1-Flag was added as an exogenous inhibitor in this assay, 100 μl DKK1-CM or 100 μl pcDNA3-CM was mixed with DMEM and FBS (to make a total volume of 250 ml containing 20% FBS) and added to each well 4 h after transfection. Cells were harvested 24 h later for determination of protein expression and luciferase activity.

**Assays involving 293T cells transfected with LRP5 and cultured in Wnt3a-containing conditioned medium.** A transfection protocol identical to the one described above was employed, except that no Wnt1-V5 construct was included among the transfected DNAs. Serum was added back to the cells 4 h after transfection. Twenty-four hours after transfection, culture medium was replaced by 100 μl of Wnt3a-CM or control L cell-CM, along with 300 μl of DMEM containing 10% FBS. When DKK1-Flag was added as an exogenous inhibitor in this assay, 70 μl DKK1-CM or 70 μl pcDNA3-CM was mixed with Wnt3a-CM or L cell-CM, DMEM, and FBS (to make a total volume of 400 μl containing 10% FBS) and added to each well 24 h after transfection. Cells were harvested 24 h later for the determination of protein expression and luciferase activity.

**Assays involving 293T cells transfected with LRP5 and cocultured with Rat2 cells stably expressing *Wnt1*.** 293T cells were plated at $1.5 \times 10^5$ cells/well in 24-well plates 24 h prior to transfection. Cells were transfected by use of Lipofectamine Plus with Topflash reporter construct (100 ng), pRL-TK (5 ng), MESD-C2 (20 ng), and full-length, untagged LRP5 (20 ng) expression vectors in 250 μl serum-free medium according to the manufacturer's protocol. After 4 h, 250 μl of DMEM containing 20% FBS was added. Twenty hours later, the medium was removed and 400 μl DMEM with 10% FBS and either $0.4 \times 10^5$ control Rat2 cells or $0.4 \times 10^5$ Rat2 cells stably expressing Wnt1 were added to each well. When DKK1-Flag was added as an exogenous inhibitor in this assay, 180 μl DKK1-CM or 180 μl pcDNA3-CM was mixed with either $0.4 \times 10^5$ control or Wnt1-expressing Rat2 cells (to make a total volume of 400 μl containing 10% FBS) and added to each well 24 h after transfection. Cells were harvested 24 h later for determination of protein expression and luciferase activity.

**Measurement of luciferase activity.** Cells were lysed in 100 μl passive lysis buffer (Promega) and firefly (Topflash) luciferase activity and *Renilla* luciferase activity were measured using the dual luciferase assay kit (Promega) in a luminometer (Molecular Devices) following the manufacturers' instructions. *Renilla* luciferase activity served as an internal control for transfection efficiency.

**Immunodetection of full-length, untagged LRP5.** Twenty microliters of cell lysate from 100 μl of passive lysis buffer was mixed with 5 μl of 5× SDS-PAGE loading buffer. Protein was resolved by SDS-PAGE under reducing conditions (5% BME), transferred to PVDF, and immunodetected by using a monoclonal anti-LRP5/LRP6 antibody 3801-100 (BioVision). As a positive control for equal cell lysate loading, immunodetection of tubulin was performed using monoclonal antibody D-10-HRP (Santa Cruz Biotechnology, Inc.).

**Coimmunoprecipitation (co-IP) of LRP5 with MESD, LRP5 with DKK1-Flag, and LRP6 with DKK1-V5.** 293T cells in 60-mm culture dishes were cotransfected with 0.5 μg LRP5-myc and 0.5 μg MESD-C2 expression vectors by use of Lipofectamine Plus. As control, 0.5 μg empty pcDNA3.1 plasmid, instead of MESD-C2, was cotransfected with LRP5-myc. Cells were lysed in 1.5 ml RIPA buffer 48 h later. Lysates were freeze-thawed once before coimmunoprecipitation was performed. A total of 0.5 ml of lysate was subjected to immunoprecipitation by the addition of 10 μl of the monoclonal anti-Flag antibody M2 (Sigma) and 50 μl protein G Sepharose beads (Amersham) and rocking at 4°C for 2 h. The beads were then washed three times in high-stringency buffer (50 mM Tris, pH 8, 150 mM NaCl, 0.5% NP-40, 0.5% Triton X-100, 0.5 mM $CaCl_2$, 0.5 mM $MgCl_2$) for 1 min each at 4°C and then pelleted and resuspended in 50 μl of 2× SDS-PAGE loading buffer containing 5% BME. Twenty microliters was then resolved by SDS-PAGE. Following transfer to PVDF, LRP5 protein was immunodetected by use of anti-myc monoclonal antibody 9E10, and MESD-C2 protein was immunodetected by use of anti-Flag antibody M2. Immunoprecipitation was also performed on 0.5 ml of lysate by adding 90 μl of the anti-myc antibody-conjugated agarose beads (9E10 AC) (Santa Cruz Biotechnology, Inc.) and rocking at 4°C for 2 h. Washes, sample electrophoresis, and immunodetection were performed as previously detailed.

For coimmunoprecipitation of LRP5N-myc and DKK1-Flag, conditioned medium containing LRP5N-myc was mixed with conditioned medium containing DKK1-Flag. Since HBM-LRP5 proteins were secreted into conditioned medium at various levels, immunodetection of secreted LRP5N-myc was first performed so that the amount of conditioned medium added for the co-IP experiments could be adjusted to provide equivalent amounts of secreted LRP5N-myc. This was accomplished by diluting aliquots of conditioned media containing the different LRP5N-myc proteins in serum free-media to a final volume of 1 ml. Fifty microliters of DKK1-Flag-containing conditioned medium was then added to the 1 ml of LRP5N-myc-containing medium, along with 10 μl of the goat anti-myc polyclonal antibody c-Myc(A-14)-G (Santa Cruz Biotechnology, Inc.) and 50 μl of protein G Sepharose beads (Amersham). Samples were rocked at 4°C for 5 h. Beads were then washed three times in low-stringency buffer (20 mM Tris, pH 7.5, 150 mM NaCl, 0.05% Tween 20) for 30 s each at 4°C and then pelleted and resuspended in 50 μl of 2× SDS-PAGE loading buffer containing 5% BME. Twenty microliters was then resolved by SDS-PAGE. Following transfer to PVDF, LRP5 protein was immunodetected by using anti-myc monoclonal antibody 9E10, and DKK1-Flag protein was immunodetected by using anti-Flag antibody M2.

For coimmunoprecipitation of LRP6N-Fc and DKK1-V5, conditioned medium containing LRP6N-Fc was mixed with conditioned medium containing DKK1-V5. LRP6N-Fc- and DKK1-V5-conditioned media were made by transiently transfecting 293T cells at 80% confluence in six-well plates with 0.8 μg LRP6N-Fc and 0.2 μg MESD-C2 expression vectors or with 1 μg DKK1-V5 expression vector, respectively, using Lipofectamine Plus. Recombinant protein in 1 ml of serum-free medium was collected 48 h later. Immunodetection of secreted LRP6N-Fc was first performed so that the amount of conditioned medium added to the mixtures in the co-IP experiments could be adjusted to provide equivalent amounts of secreted LRP6N-Fc in 1 ml of serum-free DMEM. Fifty microliters of conditioned medium containing DKK1-V5 and 50 μl of anti-mouse IgG agarose beads (Sigma) were then added. Samples were incubated at 4°C for 2 h with agitation. Beads were then washed four times in low-stringency buffer (20 mM Tris, pH 7.5, 150 mM NaCl, 0.05% Tween 20) for 1 min each at room temperature and then pelleted and resuspended in 50 μl of 2× SDS-PAGE loading buffer containing 5% BME. Twenty microliters was then resolved by SDS-PAGE. DKK1-V5 was immunodetected by using a horseradish peroxidase-conjugated monoclonal antibody against the V5 tag (Invitrogen); LRP6N-Fc was detected by using goat anti-mouse IgG antibody (Pierce). DKK1-V5 was used in these experiments instead of DKK1-Flag because the secondary antibody used to detect DKK1-Flag cross-reacted with an identically sized IgG fragment derived from the anti-mouse IgG agarose beads, making it difficult to determine whether DKK1-Flag had coprecipitated. This was not a problem when HRP-conjugated anti-V5 antibody was used.

## RESULTS

**HBM missense mutant LRP5 proteins are able to reach the cell surface.** It has previously been reported that the chaperones MESD and RAP facilitate LRP5 and LRP6 processing and targeting to the cell membrane (11). It has also been reported that the G171V HBM mutation has reduced affinity for MESD and reaches the cell surface less efficiently than wild-type protein (37). We determined the abilities of seven different HBM mutants, including G171V, to reach the cell surface. We used two approaches to evaluate LRP5 trafficking. First, we expressed a truncated LRP5 protein that lacks the transmembrane and cytoplasmic domains and is tagged with a myc epitope at the carboxy terminus (LRP5N-myc). When coexpressed with MESD, WT-LRP5N-myc was efficiently synthesized and secreted from Cos7 and 293T cells (Fig. 2A and B). When trafficked normally, WT-LRP5 (and LRP6) protein that is secreted into the culture medium is glycosylated (11) and therefore migrates on SDS-PAGE at a slightly higher molecular weight than LRP5 protein recovered from cell lysate (Fig. 2A). All HBM mutants were capable of being posttranslationally modified and secreted by Cos7 and 293T cells, albeit at differing efficiencies (Fig. 2A and B). For example, the HBM mutant proteins (D111Y, A214T, A214V, and T253I) were present in the conditioned media at levels comparable to those for WT protein, while the mutants G171R, G171V, and A242T were present in the media at significantly reduced levels (Fig. 2A and B). Importantly, the last three mutants still migrated at the larger molecular weight, indicating that they had undergone posttranslational processing prior to being secreted. Second, we expressed full-length LRP5 protein containing the transmembrane and cytoplasmic domains, again, tagged with a carboxy-terminal myc epitope, and determined their abilities to traffic to the cell surface by biotinylating cell surface proteins (Fig. 2C). The abundance of mutant protein at the cell surface (Fig. 2C) correlated with abundance of the truncated (LRP5N-myc) protein in the conditioned media (Fig. 2A and B). This result indicates that the trafficking of many HBM mutants is similar to that of WT protein and implies that abnormal trafficking and autocrine intracellular signaling do not constitute a universal mechanism for altered Wnt signaling in HBM mutations.

Because MESD is required for posttranslational modification of LRP5 and each of the HBM-LRP5 mutants appeared to be posttranslationally modified similarly to WT-LRP5, we tested the affinity between MESD and the HBM mutant proteins by coimmunoprecipitation (Fig. 3). Tagged versions of LRP5 and MESD were coexpressed in 293T cells and immunoprecipitation experiments were performed in each direction following disruption of the membranes at moderate stringency. All LRP5 mutants coprecipitated with MESD (Fig. 3); however, the affinities between the mutant forms of LRP5 and MESD did not correlate with their abilities to reach the cell surface (compare Fig. 2 and 3). For example, A242T was poorly targeted to the cell surface (Fig. 2) but had a strong affinity for MESD in this assay (Fig. 3). Conversely, A214T and T253I were efficiently trafficked (Fig. 2) but had weak affinities for MESD (Fig. 3). As previously reported (37), we found a decreased interaction between MESD and the G171V mutant.

**HBM proteins with missense mutations were not constitutively active and were able to transduce Wnt signal at rates comparable to that of WT-LRP5.** Since each of the HBM mutants reached the cell surface in different amounts and had different affinities for MESD, we tested whether they had altered abilities to transduce canonical Wnt signaling. We chose three different Wnt ligands that have previously been shown to activate canonical Wnt signaling, one of which has been implicated in the regulation of bone mass by use of transgenic and knockout mice (2). However, we do not know which, if any, of these ligands is an endogenous inducer of LRP5-mediated signaling. We assessed Wnt activation of LRP5 by transfecting the Topflash and *Renilla*-luciferase reporter constructs along with untagged, full-length WT-LRP5 or HBM-LRP5 into 293T cells that were either (i) also cotransfected Wnt1-V5 or Wnt10b, (ii) subsequently cocultured with a Rat2 cell line that stably expressed Wnt1, or (iii) subsequently cultured in medium containing Wnt3a. In the absence of Wnt, neither WT-LRP5 nor any of the HBM-LRP5 mutants was constitutively active (Fig. 4A). In all four signaling assays (i.e., cotransfection with Wnt1-V5 or Wnt10b, coculture with Wnt1 expressing cells, and addition of Wnt3a to the medium), each of the HBM mutants transduced Wnt signal at levels comparable to that for WT-LRP5 (Fig. 4A to D). For example, coexpression of Wnt1-V5 and WT-LRP5 caused a 35-fold increase in luciferase

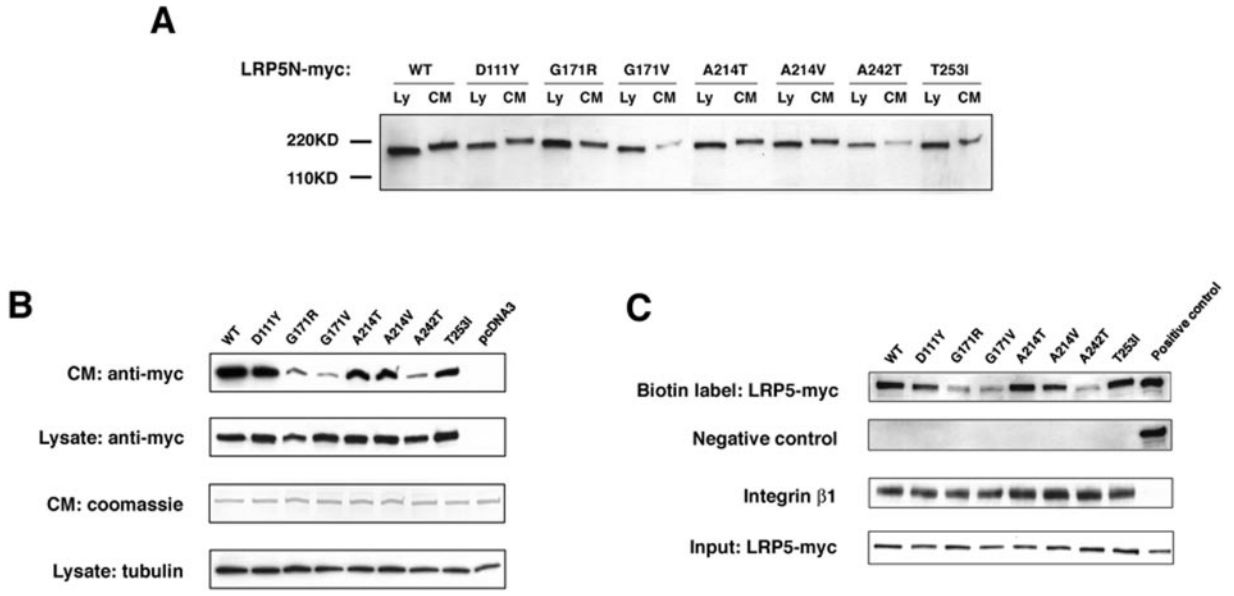


FIG. 2. Synthesis and trafficking of WT-LRP5 and seven different HBM-LRP5 mutants in transiently transfected Cos7 and 293T cells. (A) Western blot analysis of CM and cell lysate (Ly) from Cos7 cells that had been transiently transfected with LRP5N-myc constructs, separated by reducing SDS-PAGE (7.5% gel), and immunodetected by using an anti-myc antibody. Note that the molecular mass of LRP5N-myc in the conditioned medium is greater than the mass of that in the cell lysate, indicative of posttranslational modification during trafficking. Also note that the relative amounts of recombinant protein in conditioned medium in comparison to cell lysate differ between the different mutants. (B) Western blot analysis of WT and HBM-LRP5N-myc expressed in 293T cells and immunodetected after reducing SDS-PAGE (7.5% gel) with an anti-myc antibody. Comparable rates of synthesis occurred for all constructs based upon immunodetection of LRP5N-myc in the cell lysate. As with the Cos7 cells (panel A), the G171R, G171V, and A242T mutants had low abundance in CM of 293T cells compared with that in WT-LRP5N-myc. Equal loading of cell lysate and CM in each lane is demonstrated by immunodetection of cell lysate with an antitubulin antibody and Coomassie staining of conditioned medium. (C) Western blot analysis of affinity purified, biotin-labeled cell surface protein from Cos7 cells transfected with full-length LRP5-myc constructs separated by reducing SDS-PAGE (4 to 15% gradient gel) and immunodetected by using an anti-myc antibody. Note that the ability of different HBM-LRP5-myc proteins to reach the cell surface mirrors the abundance of the LRP5N-myc form of that mutant in the conditioned media of Cos7 and 293T cells (panels A and B). The negative controls comprise cell lysates from nonbiotinylated but LRP5-myc-transfected cells. The positive control in the far right column is a control for the anti-myc antibody. Integrin β1 immunodetection demonstrates equivalent biotin labeling of surface proteins between the different transfected cells. Input LRP5-myc comprises cell lysates from each of the LRP5-myc transfected cells, which demonstrates equivalent levels of expression.

activity, whereas 35-fold to 47-fold increases were observed for the HBM-LRP5 mutants (Fig. 4A). When LRP5-transfected cells were cocultured with Wnt1-expressing Rat2 cells, WT-LRP5 yielded an 11-fold increase in luciferase activity, and the HBM-LRP5 mutants yielded 10-fold to 15-fold increases (Fig. 4B). These results imply that HBM mutant proteins, including those that inefficiently transited through the cell, were still able to reach the cell surface in sufficient quantity to transduce Wnt signal comparably to WT-LRP5.

Wnt1, Wnt10b, and Wnt3a were able to activate canonical signaling in 293T cells that had not been transfected with LRP5 (Fig. 4A to D). This activation may be attributable to endogenous LRP5 and LRP6 receptors (23). Although the number of endogenous receptors on 293T cells has not been determined, their quantity in NIH 3T3 cells has been estimated to be between $10^3$ and $10^4$ per cell (1). The anti-LRP5/LRP6 antibody we utilized could not detect the endogenous LRP5 or LRP6 receptors on 293T cells (Fig. 4E, first column). Therefore, the amount of recombinant LRP5 protein expressed by transfected 293T cells (Fig. 4E) likely far exceeds the amount needed to efficiently transduce Wnt signal.

The patterns of response for the seven different HBM mutants, as assessed by induction (*n*-fold) of luciferase activity, are similar when Wnt10b and Wnt1 were transfected (compare Fig. 4D and A). This response is not solely due to transfection, since the pattern of response to exogenously added Wnt1 was similar to that of transfected Wnt1 (compare Fig. 4B and A). Interestingly, the pattern of HBM mutants' response to Wnt3a differed from that of Wnt1 or Wnt10b (compare Fig. 4C and A, B, and D). However, the Wnt3a pattern was the same whether the ligand was added exogenously or by transfection (data not shown). This result suggests that HBM mutations may cause subtle alterations in the affinities of the receptor for specific Wnt ligands.

**All HBM-LRP5 mutants were less inhibited by DKK1 than WT-LRP5.** It has previously been reported that the G171V-LRP5 mutant was less efficiently inhibited by DKK1 compared with WT-LRP5 (4). However, subsequent experiments demonstrated reduced trafficking of the G171V mutant to the cell surface and suggested that the reduced inhibition by DKK1 simply reflected there being less receptor at the cell surface; this result also suggested that the increased activity of the G171V mutant receptor was due to an intracellular interaction between the receptor and autocrine-produced Wnt ligand (37). We tested this hypothesis by adding Wnt ligand exogenously to LRP5-transfected 293T cells. All HBM mutant receptors, including G171V, were able to respond to exogenously supplied Wnt1 and Wnt3a (Fig. 4B and C), arguing against intracellular

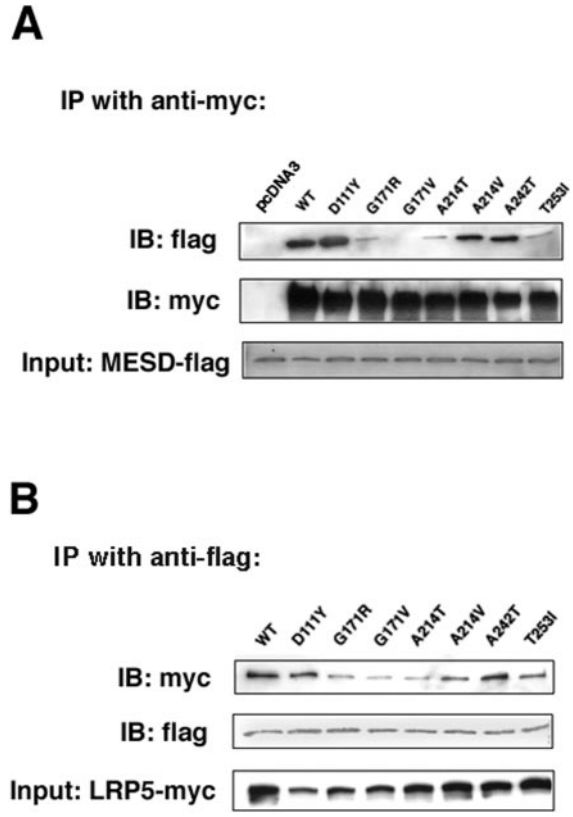


FIG. 3. HBM-causing mutations differentially affect the interaction between LRP5 and MESD-C2. Full-length LRP5-myc constructs were coexpressed with Flag-tagged MESD-C2 (MESD-flag) in 293T cells. Coimmunoprecipitation was carried out using the cell lysates. Cells that had been transfected only with MESD-Flag or LRP5-myc expression vectors served as negative controls. Cell lysate was immunoprecipitated by use of an anti-myc antibody (A) or an anti-Flag antibody (B). (A) Western blot of anti-myc-immunoprecipitated protein that was immunodetected by use of an anti-Flag antibody (IB: Flag) after reducing SDS-PAGE (4 to 15% gradient gel). Note that immunoprecipitation of WT-LRP5-myc at high stringency also precipitated MESD-Flag. Several (D111Y, A214V, and A242T) but not all HBM-LRP5-myc mutants were able to precipitate MESD-Flag at high stringency. To ensure equal immunoprecipitation of LRP5-myc proteins in the assay, LRP5-myc was immunodetected on the same blot by use of the anti-myc antibody (IB: myc). To ensure equal expression of MESD-Flag, cell lysates were immunodetected with anti-Flag antibody (Input: MESD-flag). MESD-Flag migrated as an ~30-kDa protein in this experiment. (B) Western blot of anti-Flag-immunoprecipitated protein, immunodetected by use of an anti-myc antibody (IB: myc) following reducing SDS-PAGE (4 to 15% gradient gel). Note that immunoprecipitation of MESD-Flag at high stringency comparably precipitated WT-LRP5-myc and several HBM mutants (D111Y, A214V, and A242T), while other HBM mutants were less efficiently precipitated. To ensure equal immunoprecipitation of MESD-Flag in the assay, MESD-Flag was immunodetected on the same blot by using the anti-Flag antibody (IB: flag). To ensure equal expression of LRP5-myc, cell lysates were immunodetected with anti-myc antibody (Input: LRP5-myc). Note that both assays identified the same HBM-LRP5-myc mutants as having affinities to MESD-Flag that are comparable to that of WT-LRP5-myc.

autocrine signaling as the likely mechanism. Also, as noted earlier, the patterns of responsiveness of the HBM mutants were the same whether Wnt1 was provided by cotransfection or by coculture (compare Fig. 4A and B).

Importantly, for all three Wnt ligands, we observed that each HBM mutant was less efficiently inhibited by exogenously added DKK1 in these assays than was WT-LRP5 (Fig. 4A to D). When cells were cotransfected with Wnt1-V5, the induction of luciferase activity was 70% inhibited by adding DKK1 to cells expressing WT-LRP5, whereas none of the seven HBM-LRP5 mutants was inhibited by more than 30% (Fig. 4A). Similar results were obtained when LRP5-transfected 293T cells were cocultured with Wnt1-expressing Rat2 cells. Exogenous DKK1 inhibited the induction of luciferase activity by 50% in cells expressing WT-LRP5 and by no more than 20% in any of the seven HBM mutant-expressing cells (Fig. 4B). Although the induction in luciferase activity in cells treated with Wnt3a-containing conditioned medium was smaller than that in cells treated with Wnt1-containing medium, cells expressing WT-LRP5 were more effectively inhibited by DKK1 than cells expressing any of the seven HBM mutants (Fig. 4C). The decreased inhibition by DKK1 in the HBM mutants was more clearly seen when Wnt10b was used as ligand (Fig. 4D), yielding results similar to those observed with the Wnt1 assays.

**HBM-LRP5 mutants had lower affinities to DKK1 than WT-LRP5.** DKK1 has previously been shown to physically interact with LRP5 and LRP6 (1, 27), leading us to hypothesize that HBM mutants have reduced interaction with DKK1. We tested this hypothesis by performing coimmunoprecipitation experiments between LRP5 and DKK1 (Fig. 5A). Human Flag-tagged DKK1 was expressed in 293T cells, and conditioned medium was mixed with conditioned medium containing secreted WT-LRP5N-myc or HBM-LRP5N-myc. For a control, we used LRP5 protein with the mutation T173M that had been identified in a patient with familial exudative vitreoretinopathy (31). Like each of the HBM mutants, this mutant is within the first EGF-like repeat domain, but it does not affect Wnt1 or Wnt10b signaling in Topflash reporter assays (our unpublished data). As shown in Fig. 5A, wild-type LRP5N-myc as well as the control T173M-LRP5N-myc comparably interacted with DKK1 protein, whereas all seven HBM-associated mutant proteins had significantly reduced interactions.

Since LRP6, a close homolog of LRP5, also directly interacts with DKK1 (23), we created a G158V allele in LRP6N-Fc, which is equivalent in amino acid residue location to the G171V allele of LRP5. In contrast to WT-LPR6N-Fc, the G158V mutant did not coprecipitate DKK1 (Fig. 5B).

## DISCUSSION

Our data support a role for LRP5 in transducing Wnt signal, since all HBM mutations retained this functional property, while OPPG-causing mutations did not (our unpublished data). That each HBM mutation remains Wnt responsive is important, since recent data indicate that LRP5 can participate in other biologic pathways (5, 19, 22, 35). In the eye, LRP5 likely acts as a coreceptor with Frizzled 4 for the ligand Norrin, since mutations in LRP5, FRZ4, and Norrin have each been associated with hereditary eye diseases that have altered growth and/or regression of the vitreal vasculature as a component feature (7, 15, 17, 31, 35). While it is formally possible that Norrin or an as yet unidentified protein could be the

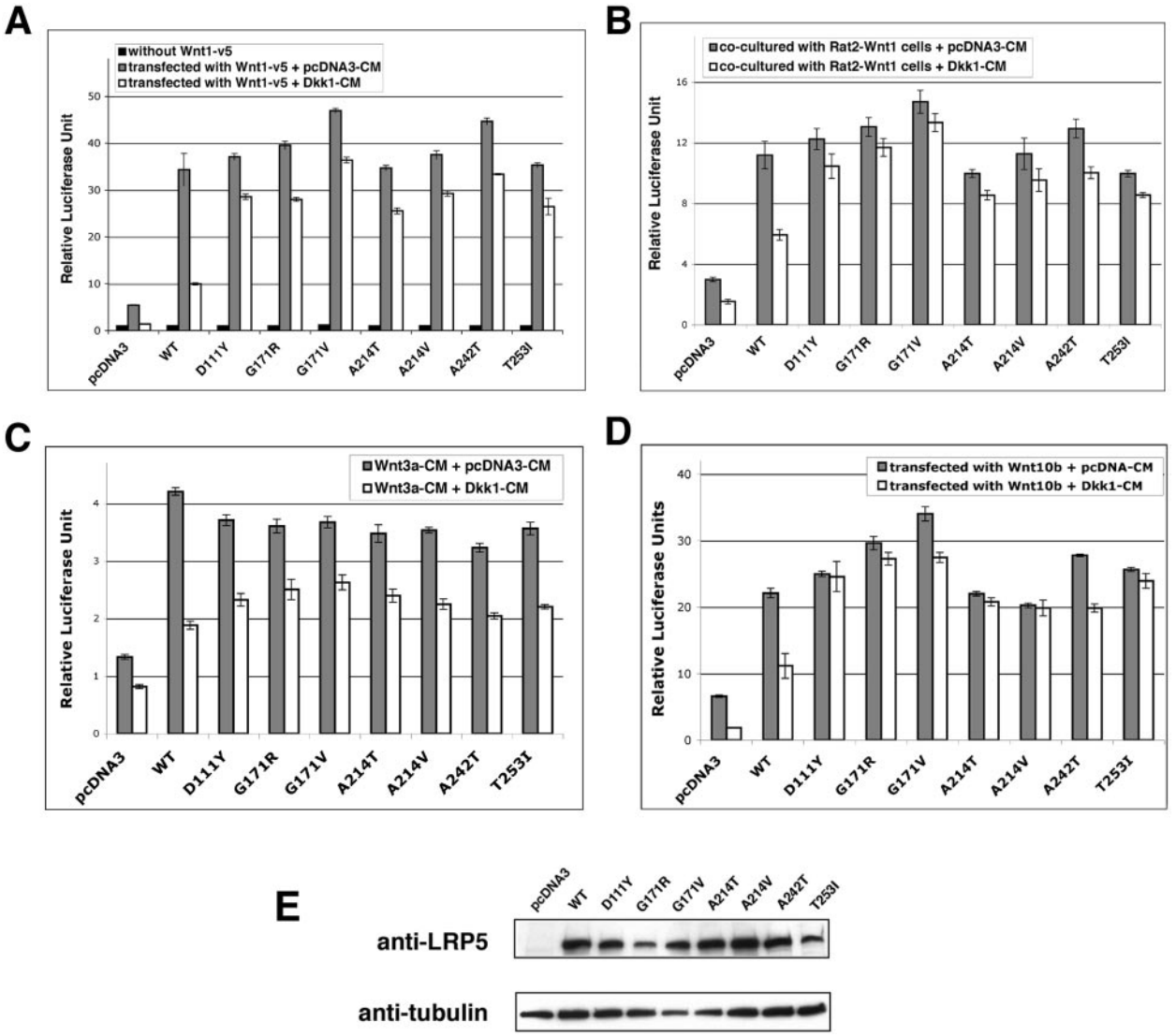


FIG. 4. Wnt-induced canonical signaling in 293T cells expressing WT-LRP5 or HBM-LRP5. Wnt-induced signaling via the canonical pathway is depicted as the increase (*n*-fold) in firefly luciferase (Topflash) activity normalized to *Renilla* luciferase activity. (A) Wnt induction by transfecting cells with LRP5 alone (black bars) or cotransfecting LRP5 with Wnt1-V5 and then culturing in the presence of pcDNA3-CM (gray bars) or DKK1-CM (open bars). (B) Wnt induction by coculturing LRP5-transfected cells with Wnt1-expressing Rat2 cells in the presence of pcDNA3-CM (shaded bars) or DKK1-CM (open bars). (C) Wnt induction by adding conditioned medium from Wnt3a-expressing L cells to LRP5-transfected cells and then culturing in the presence of pcDNA3-CM (shaded bars) or DKK1-CM (open bars). (D) Wnt induction by cotransfecting cells with LRP5 and mouse Wnt10b and then culturing in the presence of pcDNA3-CM (shaded bars) or DKK1-CM (open bars). (E) Representative Western blot of cell lysates from transfected cells separated by reducing SDS-PAGE and immunodetected with anti-LRP5 antibody, demonstrating equal levels of LRP5 expression (cell lysates from the experiment depicted in panel A are shown, but similar results were observed in all experiments). To control for equal loading, the same blot was immunodetected by antitubulin antibody. Panels A through D depict results for single experiments performed in triplicate. However, each experiment was performed on at least three separate occasions, and similar results were obtained.

principal ligand for LRP5 in bone, several lines of evidence argue against this hypothesis. Low bone mass in humans with Norrie disease, who lack Norrin (28), has not been reported, whereas it has been reported for humans and mice lacking LRP5 (7, 9, 17). Second, independent experiments involving modulation of different Wnt signaling pathway participants in mice have yielded effects upon bone mass (see, e.g., references 2, 3, and 10a).

The clustering of all HBM mutations within the first EGF-like repeat domain of the receptor implied that the mutations would share a common mechanism by which they affected signaling. Our data for six new HBM-LRP5 mutants agree with prior data for the G171V mutant (4) and indicate that this mechanism does not involve constitutive activation in the absence of ligand. This distinguishes HBM-LRP5 missense mutations from mutations in other receptors, such as PTHRP, which have been found to cause Jansen metaphyseal dysplasia as the result of constitutive activation (25, 26). We also show that all HBM-LRP5 mutants were able to transduce Wnt signal in the presence of added Wnt1 or Wnt3a. This is important

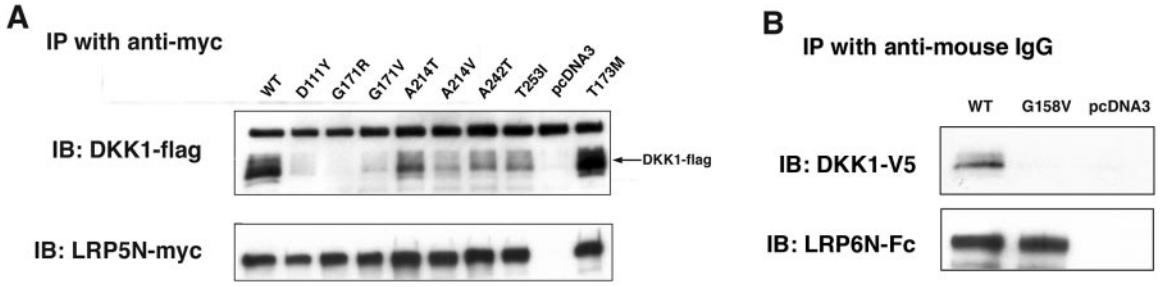


FIG. 5. All HBM-LRP5 mutants have reduced affinities for DKK1 compared to WT-LRP5. (A) Conditioned medium containing recombinant human DKK1-Flag protein was mixed with conditioned medium containing secreted LRP5N-myc or control conditioned medium from cells transfected with empty vector (pcDNA3). LRP5N-myc was immunoprecipitated from the mixed medium by use of an anti-myc antibody and coprecipitation of DKK1-Flag was immunodetected by use of an anti-Flag antibody (IB: DKK1-flag) after reducing SDS-PAGE (4 to 15% gradient gel). DKK1-Flag migrated as an ~40-kDa band in this experiment. To demonstrate equal immunoprecipitation of LRP5N-myc, the same Western blot was immunodetected with anti-myc antibody (IB: LRP5N-myc). Note that none of the HBM-LRP5N-myc proteins could coprecipitate DKK1-Flag as efficiently as WT-LRP5N-myc or the T173M-LRP5N-myc. The greater-molecular-weight immunodetectable band in all samples, including the control, is IgG heavy chain. (B) Conditioned medium containing recombinant human DKK1-V5 protein was mixed with conditioned medium containing LRP6N-Fc or control conditioned medium from cells transfected with empty vector (pcDNA3). LRP6N-Fc was immunoprecipitated by use of anti-mouse IgG agarose beads. The coprecipitated DKK1-V5 protein was immunodetected by anti-V5-HRP (IB: DKK1-V5). Equal immunoprecipitation of LRP6N-Fc protein was demonstrated by immunoblotting the same Western blot with goat anti-mouse IgG (IB: LRP6N-Fc). Note that WT-LRP6N-Fc was able to precipitate DKK1, whereas G158V-LRP6N-Fc was not.

because the Wnt interaction domain of LRP6 (and by extrapolation LRP5) is thought to involve the first and second EGF-like domains (23), and OPPG-causing missense mutations in these domains destroy the receptor's ability to transduce Wnt signal (our unpublished data). Intriguingly, we observed that several HBM-LRP5 mutants, including G171V, had greater Wnt1 and Wnt10b responsiveness than WT-LRP5 but had slightly lower Wnt3a responsiveness (Fig. 4). Consequently, it is possible that altering the affinity of the receptor to specific Wnt ligands in bone contributes to the high-bone-mass phenotype. Altered affinity of the fibroblast growth factor receptor 2 for fibroblast growth factor ligands has been implicated in causing Apert syndrome (13, 36). Other investigators did not find increased Wnt1 signal transduction by the G171V mutation compared to that of the wild type when carboxy-terminal hemagglutinin-tagged LRP5 receptors were expressed (37); however, tagging the carboxy terminus may reduce maximal signaling, since we found a carboxy-terminal myc tag impaired signaling by 50% compared to untagged receptor (our unpublished data). Therefore, the complexity of the Wnt-Frizzled-LRP signaling pathway(s) (19 different Wnt ligands, 10 different Frizzled receptors, and LRP5 and LRP6) will likely require in vivo studies using knock-in and conditional knockout alleles, rather than in vitro studies, to ultimately dissect the pathway and thereby test the validity of altered affinity to specific Wnt ligands as the mechanism for HBM-LRP5 effects.

Our results do not support the hypothesis that impaired processing of the G171V mutant and autocrine, intracellular signaling cause the HBM phenotype (37). We found that all HBM-LRP5 mutants responded similarly to Wnt1 provided either by coculture or by cotransfection (Fig. 4A and B). We also found that several HBM-LRP5s were able to transit to the cell surface (Fig. 2C) and had affinities to MESD that were similar to that of WT-LRP5 (Fig. 3). When Wnt was added to cells that had not been cotransfected with LRP5, significant canonical signaling still occurred (Fig. 4A to D), implying that endogenous LRP5 and/or LRP6 receptors transduced Wnt signal, even though they were not detectable on a Western blot (Fig. 4E). Also, the inductions (*n*-fold) of Wnt signaling were similar, whether 5 ng, 50 ng, or 100 ng of LRP5 expression constructs was transfected (our unpublished data). This suggests that components other than the transfected LRP5 receptors are rate limiting. Taken together, our results suggest that all transfected HBM-LRP5 mutants reached the cell surface in amounts sufficient to maximally transduce Wnt signal. Our results also demonstrate that the choice of Wnt ligand is important when interpreting in vitro studies of LRP5 signaling. Zhang et al. (37) attributed the difference in responsiveness between the G171V mutant and WT LRP5 to added Wnt3a, as opposed to cotransfected Wnt1, to there being less G171V mutant receptor reaching the cell surface. However, we found that exogenous Wnt3a was a less potent activator and exogenous Wnt1 was a more potent activator of several HBM mutants, independent of their efficiencies in reaching the cell surface (Fig. 4B and C).

We suggest that the reduced inhibition by DKK1 provides the most parsimonious explanation for the mechanism by which HBM-LRP5 mutations have their effects. Each HBM mutant was less inhibited by DKK1 than WT, whether stimulated by Wnt1 delivered by cotransfection or coculture (Fig. 4A and B), by cotransfected Wnt10b (Fig. 4D), or by Wnt3a added to the culture medium (Fig. 4C). We noticed that when Wnt3a was used, exogenous DKK1 inhibited HBM-LRP5 more efficiently than when exogenous Wnt1 was used (compare Fig. 4C and B). This result suggests the involvement of other factors at the cell surface (e.g., Kremens, Frizzled coreceptors, or as yet unidentified proteins) during inhibition of LRP5 by DKK1 when different Wnt ligands are present.

Our results demonstrate that in comparison to WT-LRP5, all mutant HBM-LRP5 proteins have reduced affinities to DKK1. When one HBM mutation, G171V, was introduced into an equivalent location in LRP6 (G158V), it also impaired the interaction between LRP6 and DKK1 (Fig. 5B). When first identified as an inhibitor of canonical Wnt signaling, DKK1 had been found to strongly interact with the third and fourth, but not the first and second, EGF-like domains of LRP6 (23).

For LRP5, the first two EGF-like domains or the last two domains can bind DKK1 (37). However, Wnt signaling through LRP5 protein that lacks the third and fourth domains or just the third domain could not be inhibited by DKK1, suggesting that DKK1 binding to the third propeller domain of LRP5 is critical for regulating canonical signaling (37). While our studies have not addressed the requirement of the third domain, we clearly show that perturbation within the first domain of LRP5 or LRP6 can interfere with DKK1 binding. DKK2 has also been shown to inhibit canonical Wnt signaling by binding LRP6 (23), and two other DKK family members are present in the human genome. Our results do not exclude the possibility that the HBM phenotype results from reduced inhibition by DKKs other than DKK1 or by other as yet unidentified extracellular inhibitors of LRP5.

The existence of a naturally occurring allelic series of mutations within LRP5 that caused HBM phenotypes enabled us to mutate the specific disease-associated residues and evaluate their effects upon the Wnt signaling cascade. We found that mutations at these residues consistently interfered with inhibition of the receptor by DKK1, but not with activation of the receptor by Wnt ligand, trafficking of mutant receptor to the cell surface, or interaction of the mutant receptor with intracellular chaperones. Understanding precisely how missense mutations in the first EGF-like domain impair DKK1-mediated inhibition may lead to the rational design of pharmacologic inhibitors of this pathway that can be used to effect increases in bone mass among individuals with wild-type LRP5 receptors.

## ACKNOWLEDGMENTS

We thank Xi He, Bernadette C. Holdener, Ormond A. MacDougald, Anthony M. C. Brown, and Hans Clever for sharing reagents and technical advice and Deborah Schelling, Cassandra Zylstra, Scott Robertson, and Cindy Bartels for their expert technical support.

M. L. Warman is an investigator with the Howard Hughes Medical Institute and the recipient of a Clinical Scientist in Translational Research Award from the Burroughs Wellcome Fund. Both organizations supported this work.

## REFERENCES

1. **Bafico, A., G. Liu, A. Yaniv, A. Gazit, and S. A. Aaronson.** 2001. Novel mechanism of Wnt signalling inhibition mediated by Dickkopf-1 interaction with LRP6/Arrow. Nat. Cell Biol. **3:**683–686.
2. **Bennett, C. N., K. A. Longo, W. S. Wright, L. J. Suva, T. F. Lane, K. D. Hankenson, and O. A. MacDougald.** 2005. Regulation of osteoblastogenesis and bone mass by Wnt10b. Proc. Natl. Acad. Sci. USA **102:**3324–3329.
3. **Bodine, P. V., W. Zhao, Y. P. Kharode, F. J. Bex, A. J. Lambert, M. B. Goad, T. Gaur, G. S. Stein, J. B. Lian, and B. S. Komm.** 2004. The Wnt antagonist secreted frizzled-related protein-1 is a negative regulator of trabecular bone formation in adult mice. Mol. Endocrinol. **18:**1222–1237.
4. **Boyden, L. M., J. Mao, J. Belsky, L. Mitzner, A. Farhi, M. A. Mitnick, D. Wu, K. Insogna, and R. P. Lifton.** 2002. High bone density due to a mutation in LDL-receptor-related protein 5. N. Engl. J. Med. **346:**1513–1521.
5. **Fujino, T., H. Asaba, M. J. Kang, Y. Ikeda, H. Sone, S. Takada, D. H. Kim, R. X. Ioka, M. Ono, H. Tomoyori, M. Okubo, T. Murase, A. Kamataki, J. Yamamoto, K. Magoori, S. Takahashi, Y. Miyamoto, H. Oishi, M. Nose, M. Okazaki, S. Usui, K. Imaizumi, M. Yanagisawa, J. Sakai, and T. T. Yamamoto.** 2003. Low-density lipoprotein receptor-related protein 5 (LRP5) is essential for normal cholesterol metabolism and glucose-induced insulin secretion. Proc. Natl. Acad. Sci. USA **100:**229–234.
6. **Giarre, M., M. V. Semenov, and A. M. Brown.** 1998. Wnt signaling stabilizes the dual-function protein beta-catenin in diverse cell types. Ann. N. Y. Acad. Sci. **857:**43–55.
7. **Gong, Y., R. B. Slee, N. Fukai, G. Rawadi, S. Roman-Roman, A. M. Reginato, H. Wang, T. Cundy, F. H. Glorieux, D. Lev, M. Zacharin, K. Oexle, J. Marcelino, W. Suwairi, S. Heeger, G. Sabatakos, S. Apte, W. N. Adkins, J. Allgrove, M. Arslan-Kirchner, J. A. Batch, P. Beighton, G. C. Black, R. G. Boles, L. M. Boon, C. Borrone, H. G. Brunner, G. F. Carle, B. Dallapiccola, A. De Paepe, B. Floege, M. L. Halfhide, B. Hall, R. C. Hennekam, T. Hirose, A. Jans, H. Juppner, C. A. Kim, K. Keppler-Noreuil, A. Kohlschuetter, D. LaCombe, M. Lambert, E. Lemyre, T. Letteboer, L. Peltonen, R. S. Ramesar, M. Romanengo, H. Somer, E. Steichen-Gersdorf, B. Steinmann, B. Sullivan, A. Superti-Furga, W. Swoboda, M. J. van den Boogaard, W. Van Hul, M. Vikkula, M. Votruba, B. Zabel, T. Garcia, R. Baron, B. R. Olsen, and M. L. Warman.** 2001. LDL receptor-related protein 5 (LRP5) affects bone accrual and eye development. Cell **107:**513–523.
8. **He, X., M. Semenov, K. Tamai, and X. Zeng.** 2004. LDL receptor-related proteins 5 and 6 in Wnt/beta-catenin signaling: arrows point the way. Development **131:**1663–1677.
9. **Holmen, S. L., T. A. Giambernardi, C. R. Zylstra, B. D. Buckner-Berghuis, J. H. Resau, J. F. Hess, V. Glatt, M. L. Bouxsein, M. Ai, M. L. Warman, and B. O. Williams.** 2004. Decreased BMD and limb deformities in mice carrying mutations in both Lrp5 and Lrp6. J. Bone Miner. Res. **19:**2033–2040.
10. **Holmen, S. L., A. Salic, C. R. Zylstra, M. W. Kirschner, and B. O. Williams.** 2002. A novel set of Wnt-Frizzled fusion proteins identifies receptor components that activate beta-catenin-dependent signaling. J. Biol. Chem. **277:**34727–34735.

10a. **Holmen, S. L., C. R. Zylstra, A. Mukherjee, R. E. Sigler, M. C. Faugere, M. L. Bouxsein, L. Deng, T. L. Clemens, and B. O. Williams.** Essential role of β-catenin in post natal bone acquisition. J. Biol. Chem., in press.

11. **Hsieh, J. C., L. Lee, L. Zhang, S. Wefer, K. Brown, C. DeRossi, M. E. Wines, T. Rosenquist, and B. C. Holdener.** 2003. Mesd encodes an LRP5/6 chaperone essential for specification of mouse embryonic polarity. Cell **112:**355–367.
12. **Hu, H., M. J. Hilton, X. Tu, K. Yu, D. M. Ornitz, and F. Long.** 2005. Sequential roles of Hedgehog and Wnt signaling in osteoblast development. Development **132:**49–60.
13. **Ibrahimi, O. A., A. V. Eliseenkova, A. N. Plotnikov, K. Yu, D. M. Ornitz, and M. Mohammadi.** 2001. Structural basis for fibroblast growth factor receptor 2 activation in Apert syndrome. Proc. Natl. Acad. Sci. USA **98:**7182–7187.
14. **Jeon, H., W. Meng, J. Takagi, M. J. Eck, T. A. Springer, and S. C. Blacklow.** 2001. Implications for familial hypercholesterolemia from the structure of the LDL receptor YWTD-EGF domain pair. Nat. Struct. Biol. **8:**499–504.
15. **Jiao, X., V. Ventruto, M. T. Trese, B. S. Shastry, and J. F. Hejtmancik.** 2004. Autosomal recessive familial exudative vitreoretinopathy is associated with mutations in LRP5. Am. J. Hum. Genet. **75:**878–884.
16. **Johnson, M. L., K. Harnish, R. Nusse, and W. Van Hul.** 2004. LRP5 and Wnt signaling: a union made for bone. J. Bone Miner. Res. **19:**1749–1757.
17. **Kato, M., M. S. Patel, R. Levasseur, I. Lobov, B. H. Chang, D. A. Glass II, C. Hartmann, L. Li, T. H. Hwang, C. F. Brayton, R. A. Lang, G. Karsenty, and L. Chan.** 2002. Cbfa1-independent decrease in osteoblast proliferation, osteopenia, and persistent embryonic eye vascularization in mice deficient in Lrp5, a Wnt coreceptor. J. Cell Biol. **157:**303–314.
18. **Kelly, O. G., K. I. Pinson, and W. C. Skarnes.** 2004. The Wnt co-receptors Lrp5 and Lrp6 are essential for gastrulation in mice. Development **131:**2803–2815.
19. **Kim, D. H., Y. Inagaki, T. Suzuki, R. X. Ioka, S. Z. Yoshioka, K. Magoori, M. J. Kang, Y. Cho, A. Z. Nakano, Q. Liu, T. Fujino, H. Suzuki, H. Sasano, and T. T. Yamamoto.** 1998. A new low density lipoprotein receptor related protein, LRP5, is expressed in hepatocytes and adrenal cortex, and recognizes apolipoprotein E. J. Biochem. (Tokyo) **124:**1072–1076.
20. **Korinek, V., N. Barker, P. J. Morin, D. van Wichen, R. de Weger, K. W. Kinzler, B. Vogelstein, and H. Clevers.** 1997. Constitutive transcriptional activation by a beta-catenin-Tcf complex in APC-/- colon carcinoma. Science **275:**1784–1787.

20a. **Li J., I. Sarosi, S. E. Morony, D. Hill, Y. Wang, W. Qiu, S. Adamu, M. Grisanti, K. Hoffmann, T. Gyuris, H. Nguyen, R. Cattley, P. J. Kostenuik, S. S. Simonet, and D. L. Lacey.** 2004. Transgenic mice over-expressing Dkk-1 in osteoblasts develop osteoporosis. J. Bone Miner. Res. **19**(Suppl. 1)**:**S2–S543. Abstract 1017.)

21. **Little, R. D., J. P. Carulli, R. G. Del Mastro, J. Dupuis, M. Osborne, C. Folz, S. P. Manning, P. M. Swain, S. C. Zhao, B. Eustace, M. M. Lappe, L. Spitzer, S. Zweier, K. Braunschweiger, Y. Benchekroun, X. Hu, R. Adair, L. Chee, M. G. FitzGerald, C. Tulig, A. Caruso, N. Tzellas, A. Bawa, B. Franklin, S. McGuire, X. Nogues, G. Gong, K. M. Allen, A. Anisowicz, A. J. Morales, P. T. Lomedico, S. M. Recker, P. Van Eerdewegh, R. R. Recker, and M. L. Johnson.** 2002. A mutation in the LDL receptor-related protein 5 gene results in the autosomal dominant high-bone-mass trait. Am. J. Hum. Genet. **70:**11–19.
22. **Magoori, K., M. J. Kang, M. R. Ito, H. Kakuuchi, R. X. Ioka, A. Kamataki, D. H. Kim, H. Asaba, S. Iwasaki, Y. A. Takei, M. Sasaki, S. Usui, M. Okazaki, S. Takahashi, M. Ono, M. Nose, J. Sakai, T. Fujino, and T. T. Yamamoto.** 2003. Severe hypercholesterolemia, impaired fat tolerance, and advanced atherosclerosis in mice lacking both low density lipoprotein receptor-related protein 5 and apolipoprotein E. J. Biol. Chem. **278:**11331–11336.
23. **Mao, B., W. Wu, Y. Li, D. Hoppe, P. Stannek, A. Glinka, and C. Niehrs.** 2001. LDL-receptor-related protein 6 is a receptor for Dickkopf proteins. Nature **411:**321–325.
24. **Mao, J., J. Wang, B. Liu, W. Pan, G. H. Farr III, C. Flynn, H. Yuan, S.**

**Takada, D. Kimelman, L. Li, and D. Wu.** 2001. Low-density lipoprotein receptor-related protein-5 binds to Axin and regulates the canonical Wnt signaling pathway. Mol. Cell **7:**801–809.
25. **Parfitt, A. M., E. Schipani, D. S. Rao, W. Kupin, Z. H. Han, and H. Juppner.** 1996. Hypercalcemia due to constitutive activity of the parathyroid hormone (PTH)/PTH-related peptide receptor: comparison with primary hyperparathyroidism. J. Clin. Endocrinol. Metab. **81:**3584–3588.
26. **Schipani, E., K. Kruse, and H. Juppner.** 1995. A constitutively active mutant PTH-PTHrP receptor in Jansen-type metaphyseal chondrodysplasia. Science **268:**98–100.
27. **Semenov, M. V., K. Tamai, B. K. Brott, M. Kuhl, S. Sokol, and X. He.** 2001. Head inducer Dickkopf-1 is a ligand for Wnt coreceptor LRP6. Curr. Biol. **11:**951–961.
28. **Sims, K. B.** 14 May 2004, posting date. NDP-related retinopathies. Gene Rev. [Online.].
29. **Tamai, K., M. Semenov, Y. Kato, R. Spokony, C. Liu, Y. Katsuyama, F. Hess, J. P. Saint-Jeannet, and X. He.** 2000. LDL-receptor-related proteins in Wnt signal transduction. Nature **407:**530–535.
30. **Tian, E., F. Zhan, R. Walker, E. Rasmussen, Y. Ma, B. Barlogie, and J. D. Shaughnessy, Jr.** 2003. The role of the Wnt-signaling antagonist DKK1 in the development of osteolytic lesions in multiple myeloma. N. Engl. J. Med. **349:**2483–2494.
31. **Toomes, C., H. M. Bottomley, R. M. Jackson, K. V. Towns, S. Scott, D. A. Mackey, J. E. Craig, L. Jiang, Z. Yang, R. Trembath, G. Woodruff, C. Y. Gregory-Evans, K. Gregory-Evans, M. J. Parker, G. C. Black, L. M. Downey, K. Zhang, and C. F. Inglehearn.** 2004. Mutations in LRP5 or FZD4 underlie the common familial exudative vitreoretinopathy locus on chromosome 11q. Am. J. Hum. Genet. **74:**721–730.
32. **Van Wesenbeeck, L., E. Cleiren, J. Gram, R. K. Beals, O. Benichou, D. Scopelliti, L. Key, T. Renton, C. Bartels, Y. Gong, M. L. Warman, M. C. De Vernejoul, J. Bollerslev, and W. Van Hul.** 2003. Six novel missense mutations in the LDL receptor-related protein 5 (LRP5) gene in different conditions with an increased bone density. Am. J. Hum. Genet. **72:**763–771.
33. **Wehrli, M., S. T. Dougan, K. Caldwell, L. O'Keefe, S. Schwartz, D. Vaizel-Ohayon, E. Schejter, A. Tomlinson, and S. DiNardo.** 2000. *arrow* encodes an LDL-receptor-related protein essential for Wingless signalling. Nature **407:**527–530.
34. **Whyte, M. P., W. H. Reinus, and S. Mumm.** 2004. High-bone-mass disease and LRP5. N. Engl. J. Med. **350:**2096–2099.
35. **Xu, Q., Y. Wang, A. Dabdoub, P. M. Smallwood, J. Williams, C. Woods, M. W. Kelley, L. Jiang, W. Tasman, K. Zhang, and J. Nathans.** 2004. Vascular development in the retina and inner ear: control by Norrin and Frizzled-4, a high-affinity ligand-receptor pair. Cell **116:**883–895.
36. **Yu, K., A. B. Herr, G. Waksman, and D. M. Ornitz.** 2000. Loss of fibroblast growth factor receptor 2 ligand-binding specificity in Apert syndrome. Proc. Natl. Acad. Sci. USA **97:**14536–14541.
37. **Zhang, Y., Y. Wang, X. Li, J. Zhang, J. Mao, Z. Li, J. Zheng, L. Li, S. Harris, and D. Wu.** 2004. The LRP5 high-bone-mass G171V mutation disrupts LRP5 interaction with Mesd. Mol. Cell. Biol. **24:**4677–4684.